



# Electrooptic Kerr effect of porphyrin H-aggregates in polymer films: Polymer specific spectral blue shift



Masaya Suzuki<sup>a</sup>, Kazuaki Nakata<sup>b</sup>, Reiko Kuroda<sup>c</sup>, Takayoshi Kobayashi<sup>b,d</sup>, Eiji Tokunaga<sup>a,\*</sup>

<sup>a</sup> Department of Physics, Faculty of Science, Tokyo University of Science, 1-3 Kagurazaka, Shinjuku-ku, Tokyo 162-8601, Japan

<sup>b</sup> CREST, Japan Science and Technology Agency, 4-1-8, Honcho, Kawaguchi, Saitama 332-0012, Japan

<sup>c</sup> Research Institute for Science & Technology, Tokyo University of Science, 2641 Yamazaki, Noda-shi, Chiba-ken 278-8510, Japan

<sup>d</sup> Advanced Ultrafast Laser Research Center, The University of Electro-Communications, 1-5-1, Chofugaoka, Chofu, Tokyo 182-8585, Japan

## ARTICLE INFO

### Article history:

Received 4 January 2016

In final form 11 February 2016

Available online 17 February 2016

### Keywords:

Electrooptic Kerr effect

J-aggregates

H-aggregates

Electroabsorption

Circular dichroism

Porphyrin

## ABSTRACT

J- and H-aggregates of porphyrin molecules (TPPS<sub>4</sub>) in spin-coated polymer films have been studied by electroabsorption and circular dichroism (CD) spectroscopy. A spectral blue shift of the H-band due to the electrooptic Kerr effect was observed for the first time. This occurs only for a polyvinylpyrrolidone (PVP) film, with negligibly small spectral shift observed in polyvinyl alcohol (PVA), polyvinyl sulfate (PVS), and polyacrylic acid (PAA) films, in contrast to the red shift of the J-band which is commonly observed for any host polymers. Accordingly, the CD activity in both of J- and H-bands is more enhanced in PVP films than in PVA films. The mechanism of the blue and red shifts of the respective H- and J-bands is discussed by invoking a helical structure in micro-aggregates, which is compatible with the CD spectra, based on the molecular rearrangement model. It is proved that blue- and red-shifts occur evenly to cancel each other in the H-band if a simple helical structure is assumed, in good agreement with no spectral shifts in the H-band in PVA, PVS, and PAA films.

© 2016 Elsevier B.V. All rights reserved.

## 1. Introduction

Ionic dye molecules such as porphyrin and cyanine are aggregated in a self-organized fashion in a high concentration aqueous solution. Due to the transition-dipole transition-dipole interaction between molecules in aggregation, the absorption band is shifted. The band which exhibits a red shift is called the J band (or J-aggregates), while that exhibiting a blue shift is called the H band (or H-aggregates) [1,2]. Constituent molecules stack in an edge-to-edge configuration in J-aggregates, whereas they stack in a face-to-face structure in H-aggregates. Their absorption bands are sharpened by the formation of Frenkel excitons [3]. Because of potential applications to organic nano-materials, research on J-aggregates has been attracting extensive attention for these two decades, accompanied by nearly exponential expansion in the number of research papers.

Among many possible applications, recent development of organic solar cells including dye-sensitized solar cells highlights important roles of the J- and H-aggregate formation in the photovoltaic performance in organic solar cells [4]. Historically, formation of H-dimers was to be avoided because it quenches fluorescence in dye laser operation [5]. For organic solar cell

application, on the other hand, H-aggregate formation is sometimes favored in terms of photocurrent generation efficiency by widening the solar energy absorption bandwidth [6].

One of the major research topics on J-aggregates is their high electrooptic constants [7–13]. More than two orders-of-magnitude enhancement in the electrooptic Kerr effect compared with monomers was reported for porphyrin J-aggregates in polymer (polyvinyl alcohol) films [10,11]. As porphyrin molecules, tetraphenyl porphyrin tetrasulfonic acid (TPPS<sub>4</sub>), a type of porphyrin substitution products, was studied for the J-band in the PVA film to show a large spectral red shift, the mechanism of which was successfully discussed on the molecular rearrangement model [11,12]. On the other hand, there has been no report about the electrooptic effect of the H-aggregates in TPPS. One of the reasons of a poor list of literature may be that the H-band is partially overlapped with the monomer band to make it difficult to remove the spectral contributions of the monomers. In this paper, we have studied the electrooptic Kerr effect of TPPS J- and H-aggregates in spin-coated films of various kinds of water soluble polymers. We have found that the aggregates in PVP film show a blue shift of the H-band. We have also measured circular dichroism (CD) spectra of aggregates in PVP film in comparison with those in PVA film [14]. Although many studies have been devoted to CD properties of J-aggregates [1,15–21], most of the measurements were performed

\* Corresponding author.

in solution because artifact CD arises in the solid state measurement [14]. True CD spectra of porphyrin aggregates in solid phase without artifacts were previously measured for zinc porphyrin and TPPS<sub>3</sub> [22,23] using a Universal Chiroptical Spectrophotometer (UCS-1) which can remove artifact signals arising from macroscopic anisotropies [14]. The present paper reports CD spectra of aggregates of symmetrical porphyrin molecules TPPS<sub>4</sub> in polymer films for the first time. Based on the molecular rearrangement mechanism, an appropriate model of micro-aggregates of TPPS is proposed which is consistent with the CD spectra and the other data. For the spectral shift of the H-band to occur as well as the CD activity of the J- and H-band require that micro-aggregates must include a helical structure.

## 2. Materials

TPPS molecules in aqueous solution have two ionic structures, the free-base monomer (F monomer) at low H<sup>+</sup> concentration, and the dianion monomer (D monomer) at high H<sup>+</sup> concentration that is the diprotonated F monomer. The aggregates are built up from D monomers, which is promoted by high TPPS or proton concentration in aqueous solution [3]. Since TPPS is of a planar molecular structure to have two orthogonal transition dipole moments in the molecular plane, its aggregates have both J- and H-bands. The J- and the H-band are originated approximately from side-to-side and face-to-face association. Fig. 1(a) shows the structures of the TPPS molecule, F monomer, D monomer, and aggregates. Fig. 1(b) shows absorption spectra of F-, D-monomers and aggregates in aqueous solution. TPPS aggregates have two absorption bands originating from the B-band of TPPS D monomers (434 nm), i.e., the red-shifted J-band (490 nm) and blue-shifted H-band (424 nm).

Aggregates have a hierarchical structure [18,24–27]. Micro-aggregates, or coherent aggregates, are thought to be one-dimensional Frenkel excitons, consisting of one dimensional array of composite molecules. Macro-aggregates have a higher hierarchical

structure composed of micro-aggregates. Spectroscopic properties are mainly determined by micro-aggregates, while microscopic structures observed with a microscope or nanoscope reflect macro-aggregates [18,24–27]. To determine detailed structures of micro- and macro-aggregates has always been one of the central issues in the fundamental research of J- and H-aggregates. Recently, detailed study by X-ray and electron diffraction was performed on TPPS<sub>4</sub> J-aggregates in aqueous solution and the solution deposited and dried on a substrate [28]. The results have revealed that TPPS J-aggregates are formed from a chiral porphyrin mosaic sheet as the building block. On the sheet, the orthogonal molecular transition dipoles are coupled to make two degenerate J-bands and one H-band. Together with the AFM data [18,26,27], it is interpreted that the aggregate structure formed from the sheet in solution is a nanotube, whereas that on deposition is a long bilayered ribbon formed from the collapsed nanotube. The precise aggregate structures embedded in polymer matrices, however, are still uncertain although the building block is considered to be the same. As discussed in the present paper, electrooptic effects are closely linked to precise structures of micro- and macro-aggregates in terms of the molecular rearrangement mechanism.

## 3. Experimental methods and samples

Tetraphenyl porphyrin tetrasulfonic acid hydrate (TPPS, TCI), and polyvinylpyrrolidone (PVP, Wako), polyvinyl alcohol (PVA, Kanto Kagaku), poly(vinyl sulfate) potassium salt (PVS, Aldrich) and poly(acrylic acid) (PAA, Aldrich) were purchased and used without further purification. The molecular weight of the TPPS is 934.99. Prior to the preparation of sample films, an array of 8 interdigitated aluminum electrodes, each with a width of 0.5 mm separated by gaps of 0.5 mm, was deposited on microscope slides (borosilicate crown glass) by vacuum evaporation. 8 mg of TPPS and 40 mg of PVP were dissolved in deionized water of 20 mL. The solution was cast on the slides and spin coated at 4000 rpm

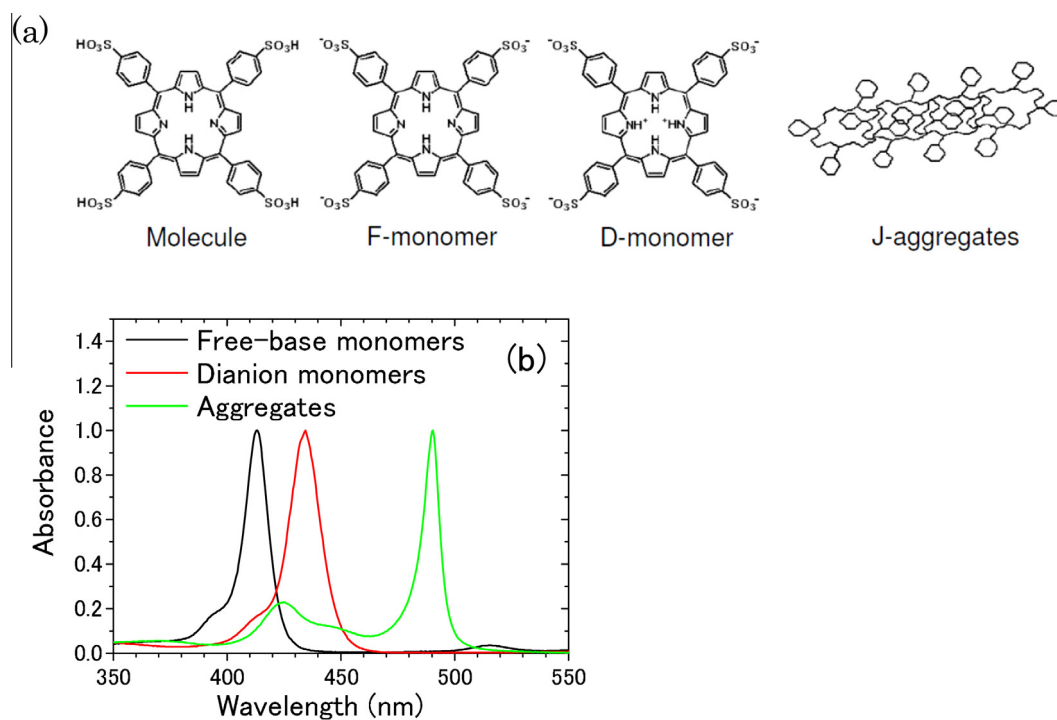


**Fig. 1.** (a) Chemical structures of the TPPS molecule, the F-monomer, and the D-monomer, and the structure of the micro-aggregate. (b) Normalized absorbance spectra of TPPS F-monomers (black), D-monomers (red), and J-aggregates (green) in aqueous solution. (For interpretation of the references to color in this figure legend, the reader is referred to the web version of this article.)

to make TPPS doped PVP films with electrodes. The rotation axis for spin coating was set about the center of the electrodes, so that there was no specific orientation of J-aggregates when averaged over the light irradiated area. TPPS PVA, PVS, and PAA films were also prepared in a similar way to the PVP films, with 8 mg TPPS and 40 mg PVA (PVS, PAA) in 20 mL deionized water.

A schematic diagram of the experimental setup for electromodulation (electroabsorption) spectroscopy is shown in Fig. 2. As a white light source, a Xe lamp (L2273, Hamamatsu Photonics) or a laser driven Xe lamp (LDLS, EQ90, Energetic Technology) was used. The unpolarized white light was focused on the sample. The transmitted light dispersed by a polychromator was transferred through a  $128 \times 16$  fiber array to and detected by 128 avalanche photodiodes. The amplified photocurrent in avalanche diodes were converted to a voltage signal with a preamplifier. The 128 voltage signals were detected with a 128 channel lock-in amplifier [29]. An AC electric field at frequency  $f$  from a function generator (FC150, Yokogawa Electric) was amplified with a high-voltage amplifier (Matsusada, HEOPT-5B20) and applied to the sample. In this way, the amplitude modulated component at the harmonic frequency  $2f$  in the transmitted light intensity was phase sensitively detected with the lock-in amplifier to obtain the transmitted light intensity change due to the Kerr effect in the samples.

The absorption spectra of the samples were measured with a spectrophotometer (UV-3101PC, Shimadzu).

A solid-state circular dichroism (CD) spectrophotometer (J-800KCM) [14] was used for measurement of CD spectra. This instrument enables us to elucidate true CD in the solid phase by canceling artifact CD due to macroscopic anisotropies such as linear birefringence and linear dichroism which are unique to the solid state.

Electrooptic parameters, the difference static polarizability  $\Delta\alpha$  and the difference electric dipole moment  $\Delta\mu$  between the excited and ground states, were evaluated by the method described in Refs. [10,11].

## 4. Results

### 4.1. Electroabsorption (EA) spectra

Fig. 3(a) shows the absorption spectrum of TPPS in PVP film. Fig. 3(b) shows the EA spectra of the J band. The Kerr signal in phase (black) was fit by the first derivative of the absorption spectrum (green) exhibiting spectral red shift. The Kerr signal out of phase (red) was fit by the second derivative of the absorption spectrum (blue) exhibiting spectral broadening. From the fitting, we obtained the difference static polarizability  $\Delta\alpha = 1100 \text{ \AA}^3$  and the difference dipole moment  $\Delta\mu = 0.095$  Debye for the J-band in PVP film.

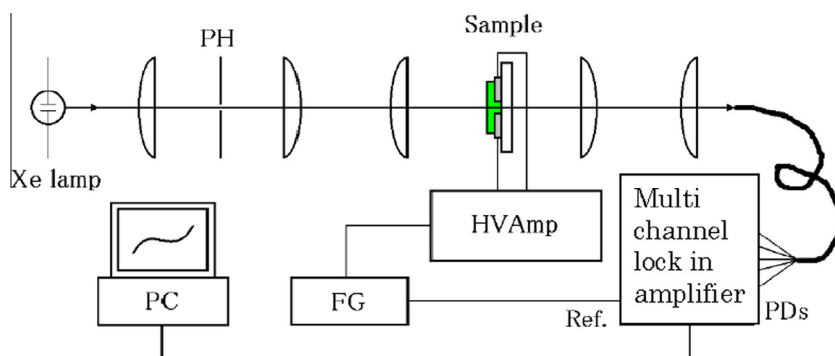


Fig. 2. Experimental setup for electromodulation (electroabsorption) spectroscopy. PH: pinhole, FG: function generator, HV Amp: high voltage amplifier, PD: photo detector.

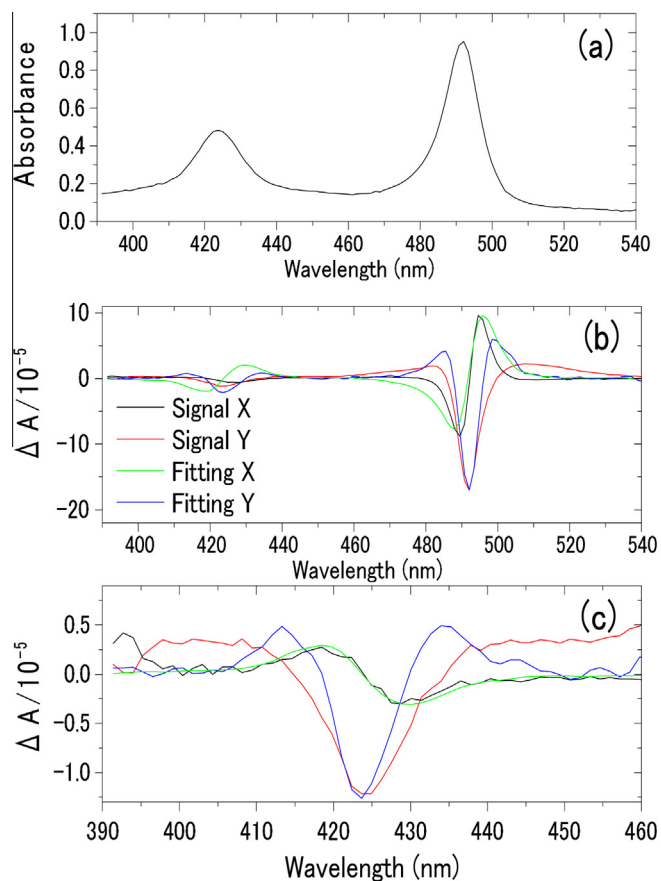


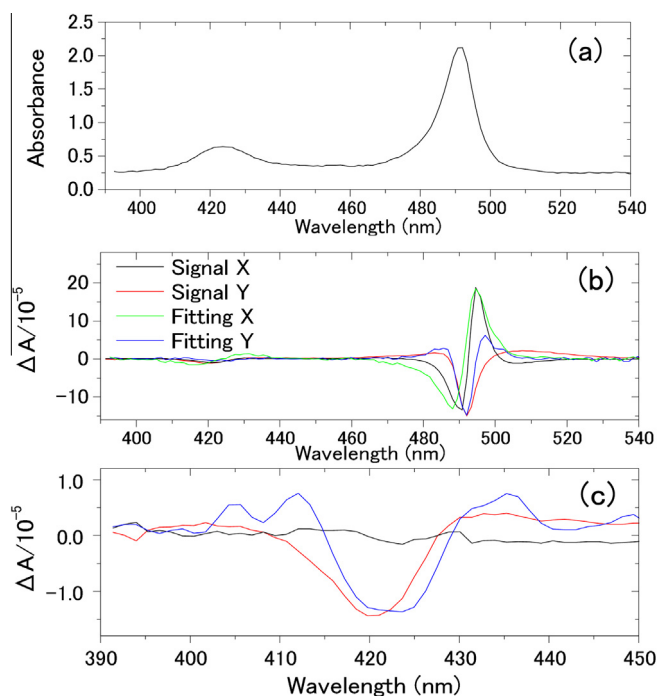
Fig. 3. (a) Absorption spectrum of TPPS in PVP film. (b) Electroabsorption spectra of TPPS in PVP film at  $2f$ , taken with the AC field magnitude of  $6.5 \times 10^5$  V/m at  $f = 221$  Hz. (c) The EA signals around the H-band in (b) is magnified. Black: in phase component (X, synchronized component without phase delay) Red: out of phase (Y, quadrature) component with  $\pi/2$  phase delay Green: the first derivative of the absorption spectrum with respect to wavelength, fitted to the black curve (X). Blue: the second derivative of the absorption spectrum with respect to wavelength, fitted to the red curve (Y). In (b), the first and second derivatives are fit to the X and Y Kerr signals in the J band. In (c), the first and second derivatives are fit to the X and Y Kerr signals in the H band. \* The signal in the H band is rotated in phase by  $0.1\pi$  with respect to the signal in the J band. (For interpretation of the references to color in this figure legend, the reader is referred to the web version of this article.)

Fig. 3(c) shows the magnified EA spectra in the H band region in Fig. 3(b). In order to best separate the shifted component from the broadening component, the X and Y signals in the H band were needed to be rotated in phase by  $0.1\pi$  against those in the J band. This is, we believe, an important parameter that indicates the difference from the Kerr signals in the J band. The Kerr signal in phase

(black) was fit by the first derivative of the absorption spectrum (green) exhibiting spectral blue shift. The Kerr signal out of phase (red) was fit by the second derivative of the absorption spectrum (blue) exhibiting spectral broadening. Direction of the shift in the H band is reversed compared with the Kerr signal in phase in the J band. From the fitting, we obtained the difference static polarizability  $\Delta\alpha = -170 \text{ \AA}^3$  and the difference dipole moment  $\Delta\mu = 0.055$  Debye for the H-band in PVP film.

This is the first observation of the electrooptic signal of TPPS H-aggregates, to the best of our knowledge, which is characterized by the blue shift. The red shift observed for TPPS J-aggregates was successfully explained by the molecular rearrangement model proposed by Katsumata et al. [11,12]. The blue shift of TPPS H-aggregates, however, cannot be explained by the model as it is, as discussed later.

Fig. 4 shows the absorption and the EA spectra at  $2f$  of TPPS in PVA film. The J-band in the EA spectra exhibits a spectral shift in X and broadening in Y, while the H-band exhibits broadening in Y as well but negligibly small signal in X. That is, the Kerr signal for the spectral shift is increased in intensity in PVP compared with in PVA. This suggests that a structural difference in the aggregates arises reflecting the difference in host polymers. This is also reflected in a difference in the absorption spectra: in Fig. 5, the absorption spectra are compared between the PVP and PVA films with both normalized to the absorbance at the J-band peak. The relative absorption intensity of the H-band is larger in PVP than in PVA. Similarly to the analyses in the PVP film, we obtained



**Fig. 4.** (a) Absorption spectrum of TPPS in PVA film. (b) Electroabsorption spectra of TPPS in PVA film at  $2f$ , taken with the AC field magnitude of  $6.5 \times 10^5$  V/m at  $f = 221$  Hz. (c) The EA signals around the H-band in (b) is magnified. Black: in phase component (X, synchronized component without phase delay). Red: out of phase (Y, quadrature) component with  $\pi/2$  phase delay. Green: the first derivative of the absorption spectrum with respect to wavelength, fitted to the black curve (X). Blue: the second derivative of the absorption spectrum with respect to wavelength, fitted to the red curve (Y). In (b), the first and second derivatives are fit to the X and Y Kerr signals in the J band. In (c), the first and second derivatives are fit to the X and Y Kerr signals in the H band. \* The signal in the H band is rotated in phase by  $0.2\pi$  with respect to the signal in the J band. (For interpretation of the references to color in this figure legend, the reader is referred to the web version of this article.)

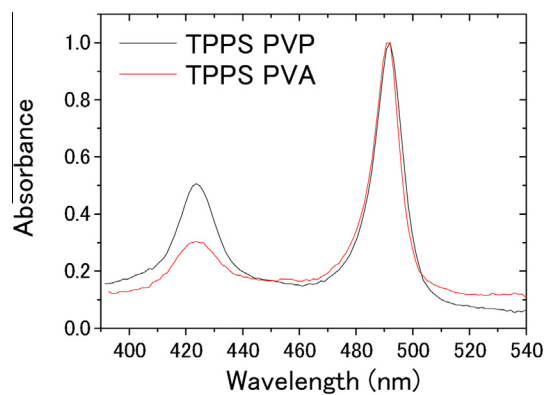


**Fig. 5.** Absorption spectra of TPPS PVP film (black) and TPPS PVA film (red), normalized to the peak intensity of the J-band.

$\Delta\alpha = 1900 \text{ \AA}^3$  and  $\Delta\mu = 0.065$  Debye for the J-band in PVA film, and  $\Delta\mu = 0.23$  Debye for the H-band in PVA film.

EA was measured also for TPPS spin-coated polymer films with other water soluble polymer materials, PVS and PAA, but no spectral shift in the H-band was observed at  $2f$  as in the case of the TPPS PVA films.

#### 4.2. Applied electric field intensity dependence

Fig. 6 shows the applied electric field intensity dependence of the amount of the spectral shift in the J- and H-bands in the X EA Kerr signal from the TPPS PVP films at the modulation frequency of 221 Hz. Fig. 6(a) and (b) shows the field intensity dependence of, respectively, the red shift in the J-band and the blue shift in the H-band. The amount of shift for both J- and H-bands increases with the field intensity to result eventually in saturation. The saturation behavior in the signal is explained by the molecular rearrangement model because there is a limit in the angle change of the transition dipole moment of TPPS molecules with respect to the applied field direction. For the EA spectra of the monomers, by contrast, the Kerr signal intensity increases without saturation up to  $4 \times 10^6$  V/m, according to Ref. [11]. This is because the signal of the monomers is due to the electronic response [11]. That is why the monomers can respond to a higher electric field than in the molecular rearrangement mechanism, where molecular orientation itself changes. This applied field intensity dependence strongly supports the signal in the H-band is caused by the same mechanism for the signal in the J-band.

#### 4.3. Modulation-frequency dependence

Fig. 7 shows the modulation-frequency dependence of the spectral shift in the quadratic electromodulation signal X in the TPPS PVP films, performed at the applied field intensity of  $F = 1.2 \times 10^6$  V/m. The amount of the red shift in the J-band and that of the blue shift in the H-band as a function of the modulation frequency of the applied field are displayed in Fig. 7(a) and (b), respectively. Both signal intensities are decreased exponentially with the frequency. This behavior is explained by the molecular rearrangement model as well, since the response time of the molecular orientational change should be restricted by the moment of inertia and the friction with host polymers.

It should be remarked that the blue shift in the H-band decreases more slowly in magnitude with frequency than the red shift in the J-band. In terms of the molecular rearrangement model, this behavior might indicate that the moment of inertia for molecular

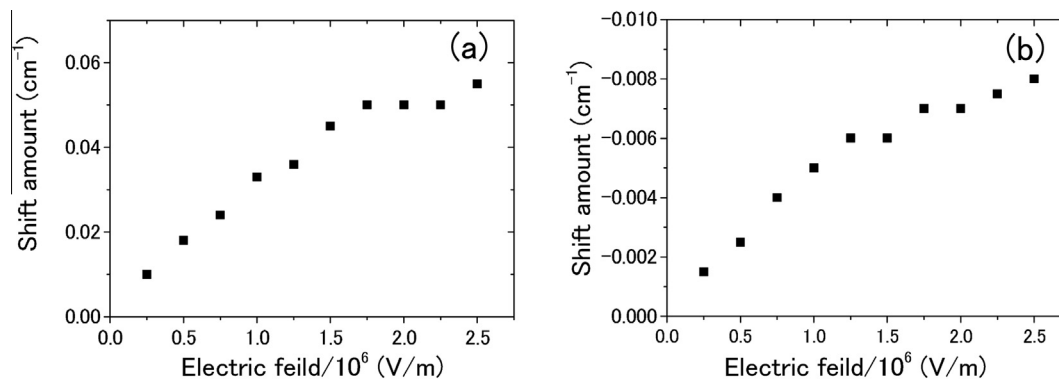


Fig. 6. Electric-field intensity dependence of the spectral shift in TPPS PVP films. (Kerr signal in X phase) (a) J-band. (b) H-band.

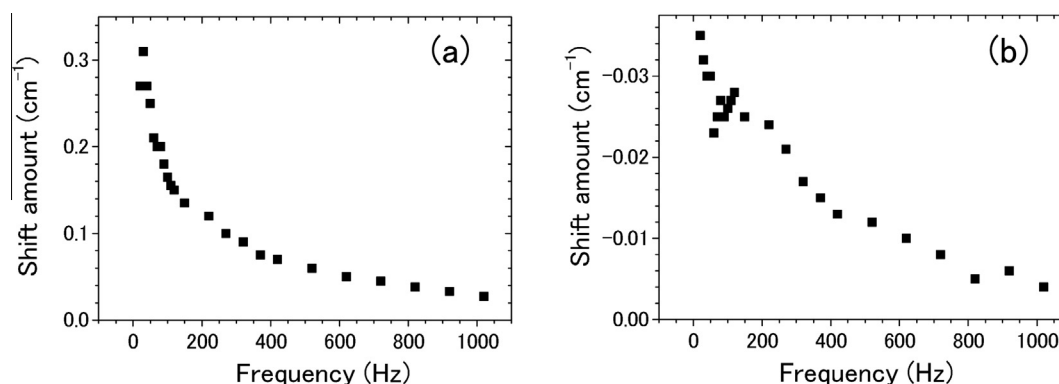


Fig. 7. Modulation-frequency dependence of the spectral shift in TPPS PVP films. (Kerr signal in X phase) (a) J-band. (b) H-band.

rotational motion causing the shift in the H-band is smaller than that in the J-band.

#### 4.4. CD spectra

Fig. 8 shows the absorbance and CD spectra of TPPS PVP and PVA films. TPPS dispersed in other matrix showed substantial apparent CD spectra, but these were due to artifact signals and hence almost zero CD intensities were obtained after our procedure of removing artefact signals (data not shown). The CD signals shown in Fig. 8 were proven to be true CD signals. While the absorption intensity is almost the same, the CD activity is about 3 times larger in the TPPS PVP film than in the TPPS PVA film. This indicates that a chiral structure in the aggregates is more strengthened in the former than in the latter. The chiral structure is likely to be brought about by a helical structure of the aggregates, as shown by AFM image for similar but asymmetrical  $H_4TPPS_3$  [18]. This result gives strong evidence that the signal in the H-band is correlated with a helical structure of the TPPS aggregates.

## 5. Discussion

First of all, the observation that both absorption and EA spectra are dependent on the surrounding polymer species elucidates the complexity in the aggregate structures in polymer matrices. Considering that the absorption and EA spectra which are relevant to the delocalized exciton wavefunction are mostly determined by the structure of micro-(coherent-) aggregates, it is indicative that even the chiral porphyrin mosaic sheet [28] is structurally perturbed by interaction with polymer molecules. In this paper, therefore, we will restrict our discussion to the basic one-dimensional

coherent aggregate to determine its prerequisite structure in the light of the molecular rearrangement model.

From the textbook mechanism of quantum mechanics, by application of an electric field, the transition energy between the ground state and the lowest excited state exhibits a red shift purely from the electronic origin as explained in Appendix A. This is why the TPPS monomer band exhibits a red shift purely from the electronic origin [10,11]. Porphyrin J- and H-aggregates, too, should exhibit a red shift from the electronic origin. In order to explain the experimental result in the PVP films, therefore, one needs to consider another mechanism.

The molecular rearrangement model was proposed to explain the giant electrooptic response in the molecular aggregates, which was difficult to be explained in terms of the purely electronic response in the Frenkel excitons delocalized over constituent molecules within the aggregates [11,12]. The model considers the change in the transition dipole–transition dipole interaction caused by the field induced change in the molecular orientation of the constituent molecules: the applied field induces the dipole moment in the originally neutral molecules. Then, the electric field aligns the induced dipole moment along the field. Since the field induced dipole moment and the transition dipole moment coincides in direction within the molecule, the transition dipole–transition dipole interaction is accordingly modified. When the applied field is AC, the dipole–dipole interaction energy is modulated with twice the AC frequency, resulting in the spectral shift in the Kerr signal.

The blue shift in the H-band observed in the EA spectra is most likely to be explained by the same mechanism as the red shift in the J-band, as supported by the field intensity and modulation frequency dependence. In fact, the molecular rearrangement model successfully explains many experimental facts observed for the

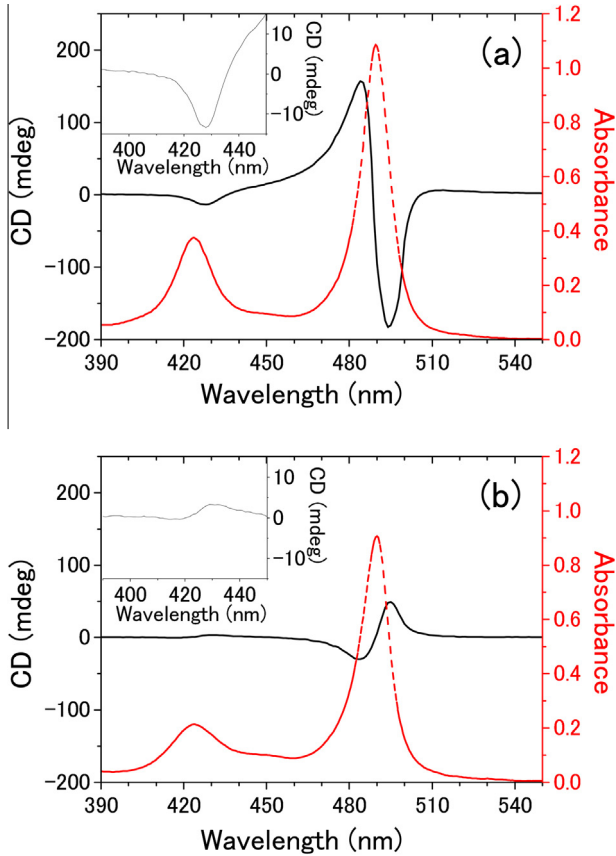


**Fig. 8.** (a) CD (black) and absorbance (red) spectra of the TPPS PVP film. Inset: magnified CD spectra for the H-band. (b) CD (black) and absorbance (red) spectra of the TPPS PVA film. Inset: magnified CD spectra for the H-band. (For interpretation of the references to color in this figure legend, the reader is referred to the web version of this article.)

red shift in the J-band. The blue shift in the H-band, however, cannot be explained with the simple molecular arrangement previously considered in the model [11]. This is because only the change in molecular axis (or molecular plane) with respect to the aggregation axis was previously considered. In order for the energy of the H-band to be affected by the field in this model, a more complicated structure in the aggregates is needed to be considered. For this purpose, we introduce a helical structure in the aggregates since it is the most likely structure among those compatible with the CD spectra.

Let us consider the transition dipole-transition dipole interaction for the molecules making a helical structure in addition to inclination of the molecular plane with respect to the aggregation axis. In the point dipole approximation, the interaction energy  $J$  between the transition dipoles of molecules separated by the distance of  $r_{ij}$  is expressed by,

$$J = \frac{1}{4\pi\epsilon_0 r_{ij}} \left[ \frac{\vec{P}_i \cdot \vec{P}_j}{r_{ij}^2} - 3 \frac{(\vec{r}_{ij} \cdot \vec{P}_i)(\vec{r}_{ij} \cdot \vec{P}_j)}{r_{ij}^4} \right] \quad (1)$$

where  $\vec{P}_i, \vec{P}_j$  are the transition dipole moment,  $\vec{r}_{ij}$  is the vector pointing from the molecule  $i$  to the molecule  $j$ , and  $\epsilon_0$  is the vacuum permittivity. Because of  $1/r^3$  dependence of the energy, it is enough to consider only the interaction of neighboring molecules.

3-Dimensional arrangement of constituent molecules in the aggregate is schematically depicted in the Cartesian coordinates in Fig. 9 in terms of the transition dipole moments along the symmetrical molecular axes. With the z-axis taken as the aggregation

axis, it is assumed that the transition dipole moment of the J-band is inclined by  $\theta$  with respect to the z-axis. For simplicity, the transition dipole moment for the H-band is assumed to be orthogonal to the aggregation axis (z-axis). Viewed from the z-axis, it is assumed that the transition dipole moments in the H-band, which are orthogonal to those in the J-band, of neighboring molecules make an angle of  $\phi$ . When the transition dipole moment in the J-band of the molecule  $i$  is on the xz plane, that in the neighboring molecule  $j$  is rotated in such a way that the y coordinate of the moment is positive, as expressed below.

$$\vec{P}_{J,i} = (P \sin \theta, 0, P \cos \theta) \quad (2)$$

$$\vec{P}_{J,j} = (P \sin \theta \cos \phi, P \sin \theta \sin \phi, P \cos \theta) \quad (3)$$

Substituting these formulas into Eq. (1), the interaction energy  $J_J$  of neighboring molecules is expressed by,

$$J_J = \frac{P^2}{4\pi\epsilon_B r^3} (\sin^2 \theta \cos \phi - 2 \cos^2 \theta) \quad (4)$$

where  $P$  is the magnitude of the transition dipole moment,  $\epsilon_B$  is the permittivity of the polymer film (background permittivity), and  $r$  is the distance between the neighboring molecules along the aggregation axis. Because of a highly symmetric structure of the TPPS molecule ( $D_{4h}$  symmetry for the D-monomer,  $H_4TPPS^{2-}$ ), the transition dipole moments in the J- and H-band are mutually orthogonal. In the present model for the aggregates, therefore, the transition dipole moment in the H-band is perpendicular to the aggregation axis (z-axis). Thus, the transition dipole moments in the H-band of neighboring TPPS molecules  $i$  and  $j$  are expressed by,

$$\vec{P}_{H,i} = (0, P, 0) \quad (5)$$

$$\vec{P}_{H,j} = (-P \sin \phi, P \cos \phi, 0) \quad (6)$$

With these formulas substituted into Eq. (1), the interaction energy  $J_H$  of neighboring molecules is expressed by,

$$J_H = \frac{P^2}{4\pi\epsilon_B r^3} \cos \phi. \quad (7)$$

To see the effect of the applied electric field on the dipole-dipole interaction, we consider the effect of  $\theta$  and  $\phi$  separately with three models as follows. Firstly, the simplest model for the aggregates to have both J- and H-bands is that with  $\theta = 0, \phi = 0$  as shown in Fig. 10(a) (model A). Next, the second simplest models are that with  $\theta \neq 0, \phi = 0$  in Fig. 10(b) (model B) and that with  $\theta = 0, \phi \neq 0$  in Fig. 10(c) (model C). The model B is used in Ref. [11] for the molecular rearrangement model and the model C is the simplest helical structure.

For each model, let us consider change in the transition-dipole transition-dipole interaction proportional to the quadratic electric field applied to the aggregates. First, the relation between the applied field direction and the aggregation axis should be characterized. Since the samples are spin-coated films on glass substrate with interdigitated electrodes, it is likely that the aggregation axes of the aggregates are oriented almost parallel to the substrate plane and are distributed isotropically on the plane. It is therefore enough to consider the field direction, which is on the plane, parallel and perpendicular to the aggregation axis. In addition, one should consider a degree of freedom for the aggregates to rotate around the aggregation axis

For the model A, the interaction energy between the neighboring TPPS molecules is expressed by,

$$J_J = -\frac{P^2}{2\pi\epsilon_B r^3} \quad (8)$$

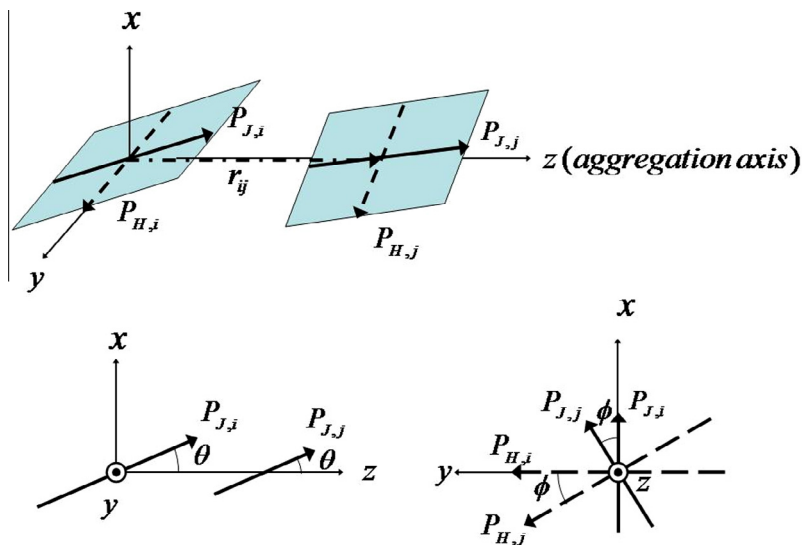


**Fig. 9.** Schematic of the model (hybrid model,  $\theta \neq 0$ ,  $\phi \neq 0$ ) for molecular arrangement in the TPPS aggregate, which considers that the molecular transition dipole moment of the J-band (thick solid arrow) is inclined against the aggregation axis (z-axis) and that the transition dipole moment in the H-band (thick dashed arrow) as well as that in the J-band is helically rotated around and along the aggregation axis. The thick solid (J) and dashed (H) arrows are mutually orthogonal, and the dashed (H) arrow is orthogonal to the z-axis. The inclination angle  $\theta$  between the transition dipole moment of the J-band and the z-axis. The rotation angle  $\phi$  between the neighboring transition dipole moment of the H-band.

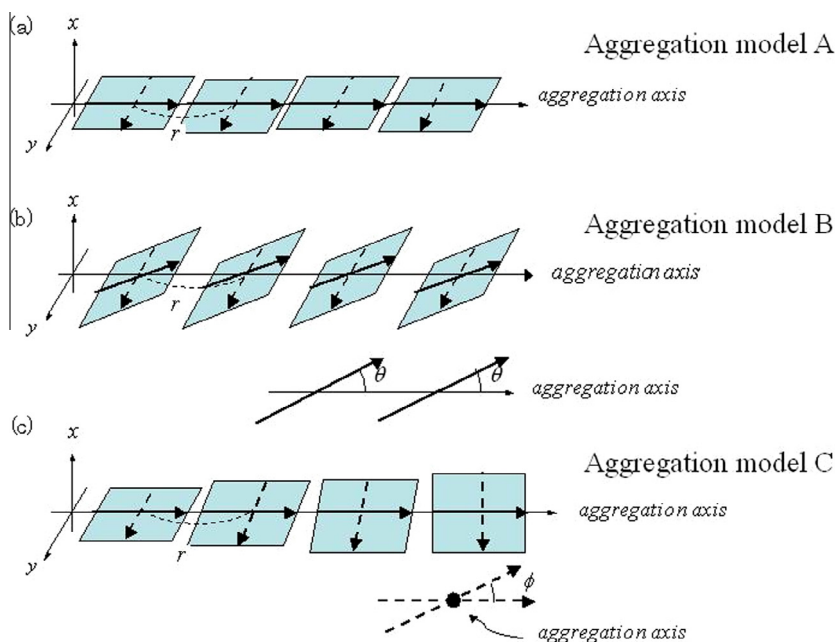


**Fig. 10.** (a) The simplest model for the TPPS aggregate to have both J- and H-bands ( $\theta = 0$ ,  $\phi = 0$ , Model A). (b) The second simplest model, where the transition dipole moment for the J-band is inclined against the aggregation axis ( $\theta \neq 0$ ,  $\phi = 0$ , Model B). (c) The simplest model with a helical structure, where only the transition dipole moment for the H-band is helically rotated around and along the aggregation axis ( $\theta = 0$ ,  $\phi \neq 0$ , Model C).

for J-aggregates and by

$$J_H = \frac{P^2}{4\pi\epsilon_B r^3} \quad (9)$$

for H-aggregates, showing that the J-band is shifted to a lower energy than the monomer band since  $J_J < 0$  while the H-band is shifted to a higher energy since  $J_H > 0$ . For the model A, configurations of the aggregates with respect to the field direction to be considered are two, as shown in Fig. 11, since all possible configurations are made by linear combinations of these two. Then, there is no change in the interaction energy in both J- and H-bands,

because the molecular orientation is not changed by the field: the torque to rotate the molecule without permanent dipole is proportional to the vector product of the field vector and the field induced electric dipole moment. Since the two molecular symmetry axes are parallel or perpendicular to the field direction, the torque is always zero.

For the model B, the interaction energy is expressed by,

$$J_J = \frac{P^2}{4\pi\epsilon_B r^3} (1 - 3 \cos^2 \theta) \quad (10)$$

for J-aggregates and

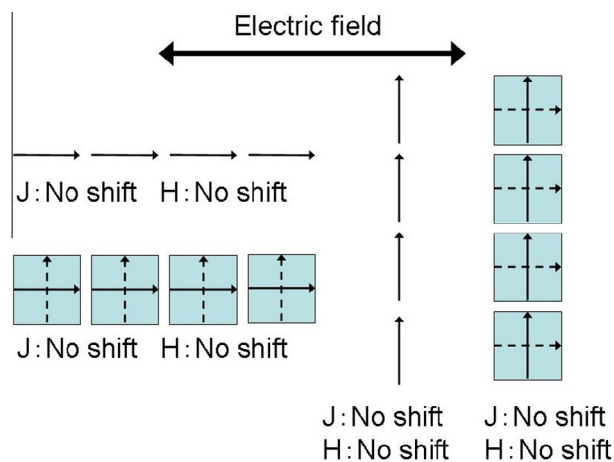


**Fig. 11.** Two possible configurations of the aggregates Model A with respect to the field direction within the spin-coated TPPS polymer film with electrodes on the glass substrate. Solid arrow: transition dipole moment of the J-band. Dashed arrow: transition dipole moment of the H-band.

$$J_H = \frac{p^2}{4\pi\epsilon_B r^3} \quad (11)$$

for H-aggregates. Here,  $\theta$  is the angle between the aggregation axis and the molecular plane.  $J_J (< 0$  for  $\theta < 54.7^\circ$ ) increases with  $\theta$  (blue shift) and decreases with decreasing  $\theta$  (red shift). For the model B, configurations of the aggregates with respect to the field direction to be considered are four, as shown in Fig. 12. For the energy change in the J-band, there are two configurations to cause a red shift and one configuration to cause a blue shift, resulting in a net red shift [11]. For the H-band, on the other hand, there is no change in the interaction energy.

For the model C, the interaction energies for J- and H-aggregates are respectively expressed by,

$$J_J = -\frac{p^2}{2\pi\epsilon_B r^3} \quad (12)$$

and

$$J_H = \frac{p^2}{4\pi\epsilon_B r^3} \cos \phi \quad (13)$$

$J_H$  decreases with  $\phi$  (red shift) and increases with decreasing  $\phi$  (blue shift). For the model C, configurations of the aggregates with respect to the field direction to be considered are two, as shown in Fig. 13. In this model, the molecular axis rotates helically along the aggregation axis such that the angle  $\phi$  is distributed uniformly over  $2\pi$ . There is no need to consider a degree of freedom of rotation around the aggregation axis. When the field direction is parallel to the aggregation axis, no change is induced. When the field direction is perpendicular to the axis, there is no change in the J-band, while there are both red shift and blue shift in the H-band. What is expected to happen in this case is schematically depicted in Fig. 14, where the aggregate of the model C is viewed from the aggregation axis direction. Since the transition dipole moment is rotated helically along the axis, the dipole moment is distributed uniformly. If the field is applied horizontally in Fig. 14, the rotational torque exerted on the induced dipole of the molecules is largest for the diagonally ( $\phi = 45^\circ$ ) oriented molecule with respect to the field direction. The magnitude of the torque decreases to zero at  $\phi = 0^\circ$  (field direction) and  $\phi = 90^\circ$  as  $\phi$  goes away from  $45^\circ$ . After the molecules are rotated,  $\Delta\phi$ , the angle between neighboring molecular axes, is smallest in the horizontal direction and largest

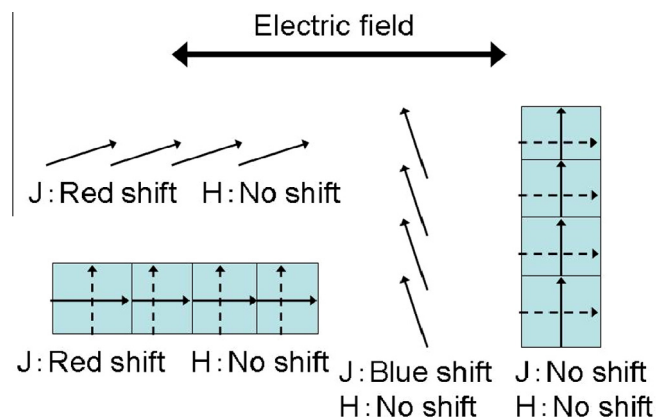


**Fig. 12.** Four possible configurations of the aggregates Model B with respect to the field direction within the spin-coated TPPS polymer film with electrodes on the glass substrate. Solid arrow: transition dipole moment of the J-band. Dashed arrow: transition dipole moment of the H-band.

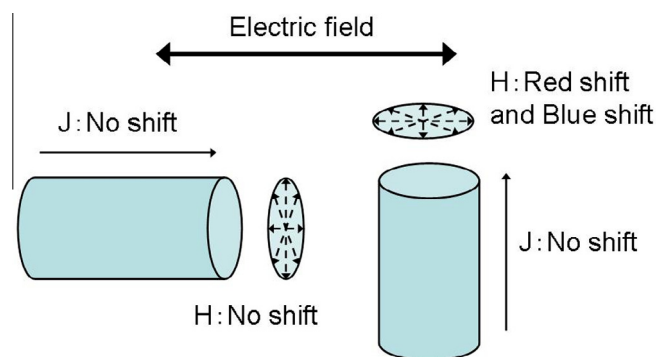


**Fig. 13.** Two possible configurations of the aggregates Model C with respect to the field direction within the spin-coated TPPS polymer film with electrodes on the glass substrate. Solid arrow: transition dipole moment of the J-band. Dashed arrow: transition dipole moment of the H-band.

in the vertical direction, if the rotated angle is assumed to be proportional to the magnitude of the torque, which is reasonable because there should be a restoring torque proportional to the angle change. As a result, there are both blue ( $\phi > 45^\circ$ ) and red ( $\phi < 45^\circ$ ) shifts induced evenly as long as an infinitesimally small angle change is considered.

The models A to C are not consistent with the CD spectra because the J-band is not CD active in all these models, whereas the intense CD activity was observed in the J-band for the TPPS PVP and PVA films. Therefore, the simplest model which is compatible with the CD spectra is that depicted in Fig. 9, the hybrid model with  $\theta \neq 0$ ,  $\phi \neq 0$  expressed by Eqs. (4) and (7). It is straightforward to prove that the hybrid model, too, blue and red shifts occurs evenly in the H-band. This result explains why TPPS in most of the polymer films (PVA, PVS, and PAA) show no detectable shift in the H-band. For the TPPS in PVP films, on the other hand, a more sophisticated model might be required to afford the blue shift in the H-band. One of the possible model is constituted by adding one more rotation  $\psi$  on the molecular plane to the hybrid model with  $\theta \neq 0$ ,  $\phi \neq 0$ . The other possibility is that the spectral shift depends critically on the higher order structure of macro-aggregates [18,26,27]. Above all, a detailed analysis based on the chiral mosaic sheet [28] is left in future study. It is, however, far from trivial to precisely predict the spectral shift on these structures.

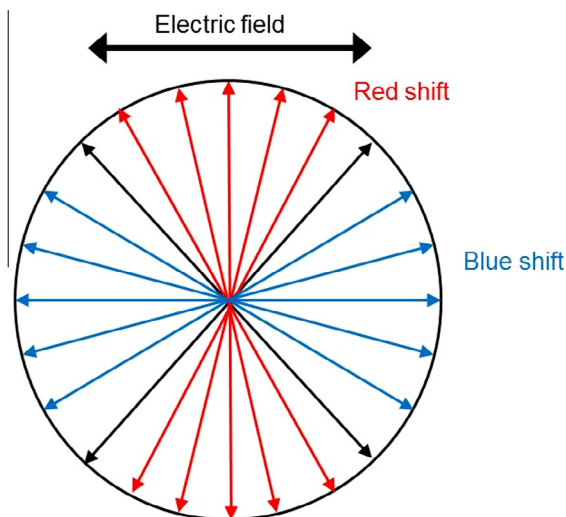


**Fig. 14.** The aggregate Model C viewed from the aggregation (z)-axis direction. From this direction, the transition dipole moment for the H-band is densely and uniformly distributed. When the field applied horizontally (field direction at  $\phi = 0^\circ$ ), the transition dipole-transition dipole interaction does not change in the diagonal direction at  $\phi = 45^\circ$ , decreases for  $\phi < 45^\circ$  (red shift), and increases for  $\phi > 45^\circ$  (blue shift) in the H-band on the approximation of infinitesimally small angle change. (For interpretation of the references to color in this figure legend, the reader is referred to the web version of this article.)

## 6. Conclusion

The electrooptic response of TPPS H-aggregates in spin coated polymer films was studied for PVA, PVS, PAA, and PVP films. For the first time, to the best of our knowledge, the blue shift in the H-band was observed in the EA spectra of the TPPS aggregates, as the Kerr effect which is proportional to the quadratic electric field applied. The blue shift was only observed for the PVP films, while there were no detectable spectral shifts observed in the H-band for the other films. The CD activity is about 3 times larger in TPPS H- and J-aggregates in PVP films than those in PVA films, strongly supporting that there is a helical structure in the micro-aggregates where the molecular axes of the constituent TPPS molecules are helically rotated around and along the aggregation axis. Even for such helical aggregates, however, blue and red shifts take place evenly to cancel each other. This agrees very well with the results for TPPS in most of the films, but requires further study on the structure of micro- and macro-aggregates in PVP films.

## Conflict of interest

There is no conflict of interest.

## Appendix A. Standard mechanism of the redshift from the electronic origin

If an electric field is applied to a molecular system, the polarization is induced by a quantum mechanical superposition state between the ground state and the higher excited states which have the parity opposite to the ground state. As a result, the nondegenerate ground state is always lowered in energy (red shift) because the coupled states are repelled by each other. This is the 2nd order Stark shift, or the electrooptic Kerr effect of purely electronic origin. The coupling strength is inversely proportional to the energy difference between the two states. Thus, if the energy difference is smaller, the red shift is larger due to stronger coupling.

From this textbook mechanism of quantum mechanics, by application of an electric field, the transition energy between the

ground state and the lowest excited state in a multilevel system almost always exhibits a red shift by the following mechanism: usually, the energy difference between the ground state and the lowest electronic excited state is much larger than those between the excited states because the density of state is increased with the energy as illustrated by the energy levels of the hydrogen atom or of a quantum well with the infinite potential barrier. Thus, the lowest excited state is lowered due to the stronger coupling with closely spaced higher excited states with the opposite parity (causing a large red shift) than the coupling with the distant ground state (causing a small blue shift). This red shift of the lowest excited state is larger than the red shift of the ground state due to the coupling with the distant excited states. Thus, the overall shift of the transition energy is usually the red shift. This is why the TPPS monomer band exhibits a red shift in the EA spectrum purely from the electronic origin.

Since the transition dipole moment in the H-band is orthogonal to that in the J-band, the relevant excited states (exciton state) for the H- and J-bands are not mutually coupled by an electric field. In addition, the delocalized exciton states including the dark states (for H-aggregates, partially allowed or forbidden states below the observed allowed H-band) are not mutually coupled by an electric field [30]. Therefore the H-band should exhibit a red shift as well purely from the electronic origin, due to the mechanism explained above. In addition, it is remarkable that the H-aggregates exhibit the blue shift despite the fact that the constituent molecules exhibit the red shift from the electronic origin [10,11].

## References

- [1] T. Kobayashi (Ed.), J-Aggregates, World Scientific, Singapore, 1996.
- [2] T. Kobayashi (Ed.), J-Aggregates, vol. 2, World Scientific, New York, 2012.
- [3] D.M. Chen, T. He, D.F. Cong, Y.H. Zhang, F.C. Liu, J. Phys. Chem. A 105 (2001) 3981.
- [4] K.C. Deing, U. Mayerhöffer, F. Würthner, K. Meerholz, Phys. Chem. Chem. Phys. 14 (2012) 8328.
- [5] D. Setiawan, A. Kazaryan, M.A. Martoprawiro, M. Filatov, Phys. Chem. Chem. Phys. 12 (2010) 11238.
- [6] A. Zitzler-Kunkel, M.R. Lenze, K. Meerholz, F. Würthner, Chem. Sci. 4 (2013) 2071.
- [7] K. Misawa, T. Kobayashi, Nonlinear Opt. 14 (1995) 103.
- [8] A. Chowdhury, S. Wachsmann-Hogiu, P.R. Bangal, I. Raheem, L.A. Peteanu, J. Phys. Chem. B 105 (2001) 12196.
- [9] A. Chowdhury, L. Yu, I. Raheem, L. Peteanu, L.A. Liu, D.J. Yaron, J. Phys. Chem. A 107 (2003) 3351.
- [10] T. Ogawa, E. Tokunaga, T. Kobayashi, Chem. Phys. Lett. 408 (2005) 186.
- [11] T. Katsumata, K. Nakata, T. Ogawa, K. Koike, T. Kobayashi, E. Tokunaga, Chem. Phys. Lett. 477 (2009) 150.
- [12] K. Nakata, T. Kobayashi, E. Tokunaga, Opt. Rev. 17 (2010) 346.
- [13] K. Nakata, T. Kobayashi, E. Tokunaga, Phys. Chem. Chem. Phys. 13 (2011) 17756.
- [14] R. Kuroda, T. Harada, Y. Shindo, Rev. Sci. Instrum. 72 (2001) 3802.
- [15] F.D. Saeva, G.R. Olin, J. Am. Chem. Soc. 99 (1977) 4848.
- [16] O. Ohno, Y. Kaizu, H. Kobayashi, J. Chem. Phys. 99 (1993) 4128.
- [17] J.M. Ribó, J. Crusats, F. Sagués, J. Claret, R. Rubires, Science 292 (2001) 2063.
- [18] C. Escudero, J. Crusats, I. Diez-Perez, Z. El-Hachemi, J.M. Ribo, Angew. Chem. 118 (2006) 8200; [Angew. Chem. Int. Ed. 45 (2006) 8032].
- [19] K. Adachi, K. Chayama, H. Watarai, Langmuir 22 (2006) 1630.
- [20] N. Micali, H. Engelkamp, P.G. van Rhee, P.C.M. Christianen, L. Monsù Scolaro, J. C. Maan, Nat. Chem. 4 (2012) 201.
- [21] A. Eisfeld, R. Kniprath, J.S. Briggs, J. Chem. Phys. 126 (104904) (2007) 1.
- [22] V.V. Borovkov, T. Harada, G.A. Hembury, Y. Inoue, R. Kuroda, Angew. Chem. Int. Ed. 42 (2003) 1746.
- [23] Z. El-Hachemi, O. Arteaga, A. Canillas, J. Crusats, C. Escudero, R. Kuroda, T. Harada, M. Rosa, J.M. Ribo, Chem. Eur. J. 14 (2008) 6438.
- [24] P.J. Reid, D.A. Higgins, P.F. Barbara, J. Phys. Chem. 100 (1996) 3892.
- [25] H. von Berlepsch, C. Bottcher, L. Dahne, J. Phys. Chem. B 104 (2000) 8792.
- [26] R. Rotomskis, R. Augulis, V. Smitka, R. Valiokas, B. Liedberg, J. Phys. Chem. B 108 (2004) 2833.
- [27] Y. Kitahama, Y. Kimura, K. Takazawa, Langmuir 22 (2006) 7600.
- [28] Z. El-Hachemi, C. Escudero, F. Acosta-Reyes, M. Teresa Casas, V. Altoe, S. Aloni, G. Oncins, A. Sorrenti, J. Crusats, J.L. Camposc, J.M. Ribó, J. Mater. Chem. C. 1 (2013) 3337.
- [29] N. Ishii, E. Tokunaga, S. Adachi, T. Kimura, H. Matsuda, T. Kobayashi, Phys. Rev. A 70 (2004) 023811.
- [30] P. Petelenz, Org. Electron. 5 (2004) 115.